Double-layered ruthenate $Sr_3Ru_2O_7F_2$ formed by fluorine insertion into $Sr_3Ru_2O_7$

R. K. Li and C. Greaves
School of Chemistry, The University of Birmingham, Edgbaston, Birmingham B15 2TT, United Kingdom
(Received 14 February 2000)

A new compound with the composition of $Sr_3Ru_2O_7F_2$ has been obtained by fluorination of the double layered Ruddlesden–Popper phase, $Sr_3Ru_2O_7$. Neutron powder diffraction (NPD) reveals that due to a similar rotation of RuO_6 octahedra, the structure of $Sr_3Ru_2O_7F_2$ can be described with the same space group *Pban* as $Sr_3Ru_2O_7$ but with a large expansion in the *c* axis and slight contraction in the *ab* plane [$a=5.4231(4)$ Å, $b=5.4168(4)$ Å, and $c=24.2505(8)$ Å, 290 K]. The fluorinated ruthenate retains the layer structure: F occupies the interstitial sites in the rock salt layer leaving the double RuO layer intact. NPD at 2 K shows that $Sr_3Ru_2O_7F_2$ is antiferromagnetic, with a *G*-type ordering of the Ru spins and an ordered moment of $\mu_z = 1\mu_B$/Ru along the *c* direction. Magnetization measurements implies a small ferromagnetic moment below 185 K, which is attributed to canting of the Ru spins from the *c* axis.

I. INTRODUCTION

Layered ruthenate compounds with the so-called Ruddlesden-Popper structure ($A_{n+1}Ru_nO_{3n+1}$) have received much attention because of their interesting electric and magnetic properties. The infinite layer $SrRuO_3$ ($n=\infty$ member) is known to be a ferromagnetic (FM) metal with an ordered moment below 165 K.[1] The recent finding of superconductivity in the $n=1$ member, Sr_2RuO_4,[2] has stimulated detailed studies of the ruthenate compounds, since it possesses the same K_2NiF_4 type structure as the high-T_c superconductor $(La,Sr)_2CuO_4$ and may be the first member of another kind of exotic superconductor.[3] The properties of the intermediate member with $n=2$ appears to depend on preparative conditions and doping. A flux grown single crystal showed FM behavior below 105 K with a large ($1.3\mu_B$/Ru) saturation magnetization,[4] while floating zone melt grown crystals and powder samples prepared by solid state reaction are paramagnetic or antiferromagnetic (AFM).[5,6] Neutron powder diffraction (NPD) study on powdered $Sr_3Ru_2O_7$ sample also failed to detect any ordered moment in excess of $0.05\mu_B$/Ru.[7]

Among the ruthenate compounds, as aforementioned, the magnetic ground state is susceptable to impurity or doping. Both the magnetism of $SrRuO_3$ and superconductivity of Sr_2RuO_4 can be easily suppressed by doping Sr with Ca. The magnetic instability of these oxides may be instrumental in forming the triplet superconducting pairing state in Sr_2RuO_4.[3] Doping Sr with Ca in the double-layer $Sr_3Ru_2O_7$ can also change its electronic ground state which spans from FM metal to AFM metal and AFM insulator.[8] This change caused by isovalent cation doping was attributed to bandwidth variation resulting from changes in Ru–O bond length and Ru–O–Ru bond angles.[5]

Band filling also has a major influence on the properties of transition metal oxides and can be achieved by aliovalent ion doping or ion insertion. Fluorine intercalation has proved to be particularly powerful for varying the physical properties of such oxides. Insertion of F into Sr_2CuO_3 produces a structural transformation and the fluorinated samples with the composition $Sr_2CuO_2F_{2+x}$ represent a new type of superconductor.[9] The fluorination of the double layered manganite $(La,Sr)_3Mn_2O_7$ with giant magnetic resistance property is also promising for chemical control of the Mn oxidation state in such materials.[10] We have found that fluorine insertion into the layered ruthenates is also possible. Since fluorination increases the valence state, while retaining the layered structure, different ground states and properties are expected for these F-containing compounds. In this paper we will report the preparation of $Sr_3Ru_2O_7F_2$ [a Ru(V) phase] from $Sr_3Ru_2O_7$ [a Ru(IV) oxide] and the results from structural and magnetic studies.

II. EXPERIMENT

The starting material $Sr_3Ru_2O_7$ was prepared from $SrCO_3$, and Ru metal powder. An excess of 1% $SrCO_3$ was

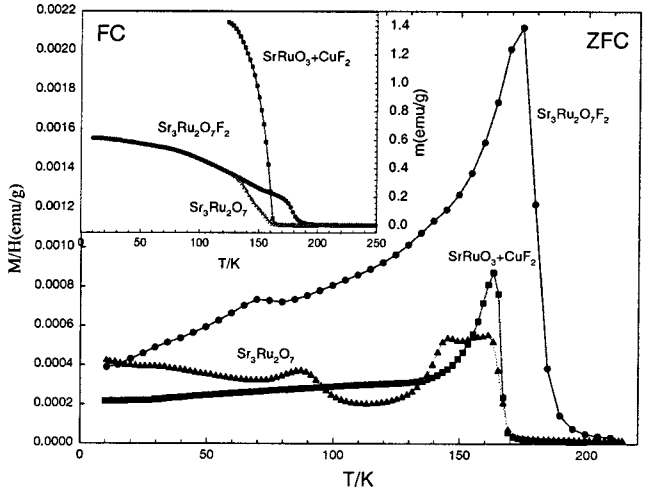

FIG. 1. Magnetic susceptibilities (ZFC) of $Sr_3Ru_2O_7F_2$, $Sr_3Ru_2O_7$, and $SrRuO_3+CuF_2$ (the inset shows the field cooled magnitizations of the samples, note the scale of the ZFC curve of $SrRuO_3$ has been reduced to $\frac{1}{20}$ and all the measurements were performed with an applied field of 200 G except for $SrRuO_3$, where the applied field is 10 G).

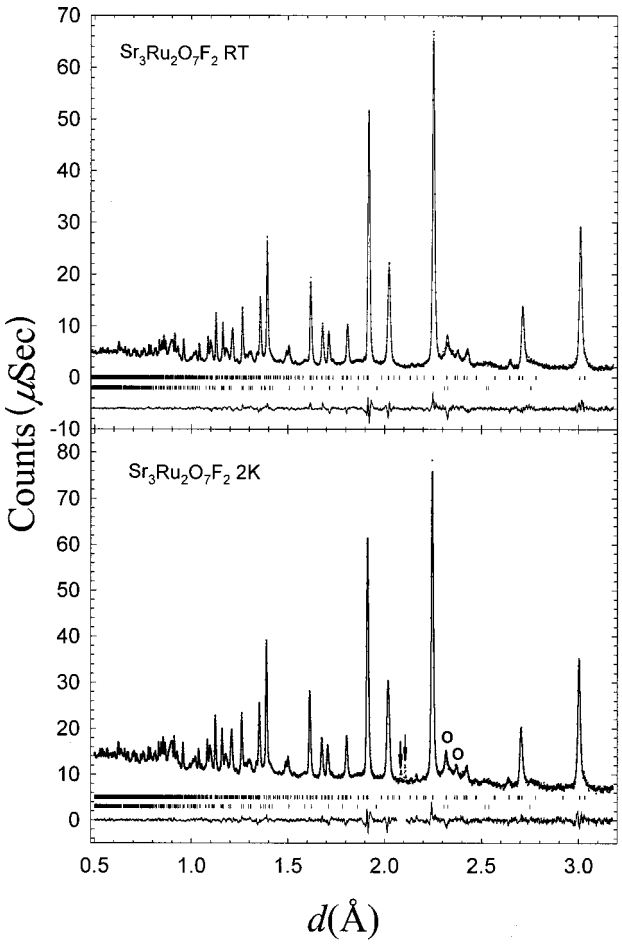

FIG. 2. Neutron diffraction patterns (C-Bank) of $Sr_3Ru_2O_7F_2$ at 290 K (top) and 2 K (bottom): (dots) observed plot, (lines) calculated and difference plot; the vertical marks represent the allowed diffraction peaks for $Sr_3Ru_2O_7F_2$ (upper) and CuO (lower). The two arrows in the 2 K pattern indicate the diffraction peaks from the cryostat, which were excluded from the refinement).

added in order to suppress the formation of ferromagnetic $SrRuO_3$. The sample was repeatedly heated up to 1400 °C in air to obtain a single phase sample based on x-ray powder diffraction (XRPD). Fluorinated samples were prepared by mixing and heating the synthesized $Sr_3Ru_2O_7$ with CuF_2 in a 1:1.02 molar ratio. The mixture was repeatedly heated for 12 h in air at temperatures rising from 220 to 300 °C. XRPD was performed with a Siemens D-5000 diffractometer equipped with a Cu $K\alpha_1$ radiation source and a position sensitive detector. Time of flight NPD data were collected at room temperature (290 K) and 2 K with the pulsed neutron source at POLARIS (ISIS, RAL, UK). Magnetization measurements were made using a Cryogenics S100 superconducting quantum interferences device susceptometer. Structure refinement was performed on the NPD data with the GSAS package.[11]

III. RESULTS AND DISCUSSION

The XRPD patterns showed that the as-synthesized sample of $Sr_3Ru_2O_7$ is single phase. All the diffraction peaks were indexed on a tetragonal unit cell, space group $I4/mmm$, and cell parameters of ($a = 3.892$ Å, $c = 20.72$ Å), which

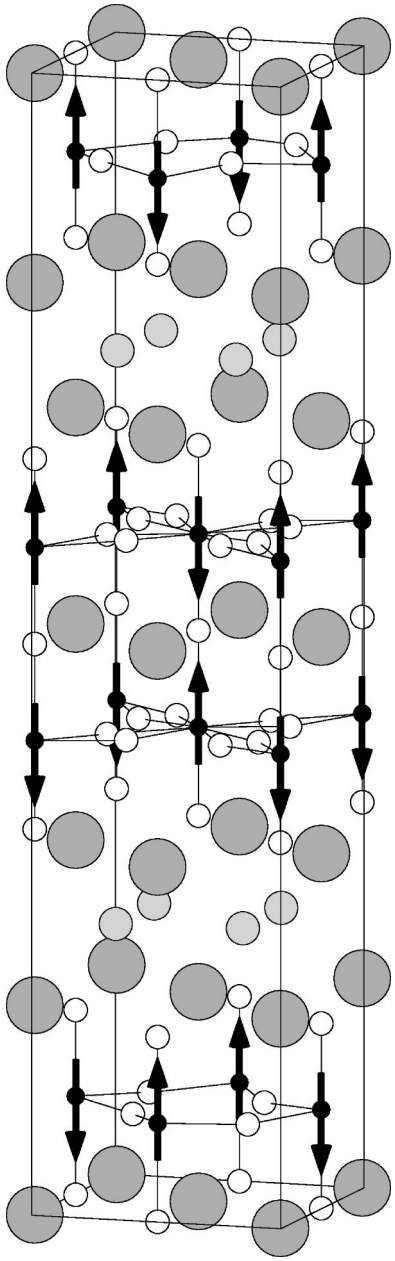

FIG. 3. Crystal and magnetic structure of $Sr_3Ru_2O_7F_2$. The large shaded circles represent Sr atoms, small open circles are oxygen, small filled circles are Ru, and medium shaded circles are fluorine.

agree with those reported in the literature. Thermal gravimetric analysis (TGA) gave an oxygen content of 7.01(3), indicating that a stoichiometric sample was obtained. The XRPD pattern of the fluorinated sample was also indexed with the same space group but with a much larger c parameter and slightly smaller a parameter ($a = 3.830$ Å, $c = 24.26$ Å).

Although XRPD patterns suggested that the samples were single phase, magnetic measurements of $Sr_3Ru_2O_7$ showed that a small amount of $SrRuO_3$ is always present to cause a rise in magnetization at 165 K (Fig. 1). This result agrees with other reports that only several ppm of $SrRuO_3$ present in the layered ruthenate material can cause a detectable FM moment at 165 K. In the zero field cooled (ZFC) magnetization curve, a second peak around 100 K is observed, which may originate from the FM transition of $Sr_3Ru_2O_7$ itself, as

TABLE I. Refined structural parameters of $Sr_3Ru_2O_7F_2$ at 290 and 2 K. Fractional occupancies n for all atoms taken as unity except for O6 and O7, where $n=0.5$.

	At 290 K Space Group: $Pban$, $a=5.4231(4)$ Å $b=5.4168(4)$ Å, $c=24.2505(8)$ Å				At 2 K Space Group: $Pban$, $a=5.4091(4)$ Å $b=5.4014(4)$ Å, $c=24.2145(7)$ Å			
Atoms	x	y	z	U_{iso}(Å^2) [a]	x	y	z	U_{iso}(Å^2) [a]
Sr1	0.25	0.25	0	0.0060(6)	0.25	0.25	0	0.0003(5)
Sr2	0.75	0.25	0.5	0.0043(5)	0.75	0.25	0.5	0.0001(4)
Sr3	0.25	0.25	0.1838(1)	0.0102(5)	0.25	0.25	0.1836(1)	0.0045(4)
Sr4	0.75	0.25	0.3107(1)	0.0114(6)	0.75	0.25	0.3104(1)	0.0060(5)
Ru1 [b]	0.75	0.25	0.0863(1)	0.0034(4)	0.75	0.25	0.0863(1)	0.0014(5)
Ru2 [b]	0.25	0.25	0.4158(1)	0.0083(6)	0.25	0.25	0.4155(1)	0.0050(6)
O1	0.75	0.25	0	0.020(2)	0.75	0.25	0	0.016(1)
O2	0.25	0.25	0.5	0.0055(8)	0.25	0.25	0.5	0.0023(7)
O3	0.75	0.25	0.1619(3)	0.019(1)	0.75	0.25	0.1616(3)	0.016(1)
O4	0.25	0.25	0.3380(3)	0.0115(8)	0.25	0.25	0.3376(2)	0.0062(7)
O5	0.4551(10)	0.0460(9)	0.0811(1)	0.0033(3)	0.4528(8)	0.0500(8)	0.0816(1)	0.0007(3)
O6 [c]	0.4434(4)	−0.0566(4)	0.4126(1)	0.0161(6)	0.4428(5)	−0.0572(5)	0.4127(2)	0.0155(6)
O7 [c]	0.5566(4)	0.0566(4)	0.4126(1)	0.0161(6)	0.5572(5)	0.0572(5)	0.4127(2)	0.0155(6)
F	0.5249(5)	0.0047(7)	0.25	0.0104(4)	0.5262(4)	0.0057(6)	0.25	0.0034(3)
R_{wp}		2.89%				1.46%		
χ^2		3.04				2.32		

[a]Mean-square atomic displacement: $U_{iso}=B_{iso}/4\pi$.
[b]$m_z=1.05(7)\mu_B$ for Ru1 and Ru2 at 2 K.
[c]Constraint by symmetry.

observed in the flux grown single crystal,[4] but only a very small magnetic moment ($\sim 0.02\mu_B$/Ru) can be seen here (Fig. 1). After fluorination, a distinct rise in the susceptibility at 185 K is observed, which indicates a FM transition at that temperature. To ensure this peak is unrelated to the FM transition of $SrRuO_3$, we have subjected a sample of $SrRuO_3$ to identical fluorinating conditions used for fluorinating $Sr_3Ru_2O_7$. The magnetization of this sample, also shown in Fig. 1, clearly shows the FM transition at 165 K, coincident with the T_c of $SrRuO_3$, but no features at higher temperatures. It is therefore clear that the transition at 185 K observed after fluorinating $Sr_3Ru_2O_7$ can be attributed to the majority phase, which has been shown (see below) to have the composition $Sr_3Ru_2O_7F_2$. The small kink at 70 K in the ZFC magnetic susceptibility curve of $Sr_3Ru_2O_7F_2$, which coincides with the spin reorientation temperature of $Sr_3Ru_2O_7$ according to Cao, McCall, and Crow,[4] may be attributed to the unfluorinated starting material $Sr_3Ru_2O_7$ or $SrRuO_3$ contained in the sample.

Structure refinements were performed using the neutron diffraction data. The high resolution C-bank ($2\theta=145°$ backscattering) and the wide range A-bank ($2\theta=35°$) data were used simultaneously. Several small peaks around $d=2.32$ Å and $d=2.37$ Å were inconsistent with the space group $I4/mmm$. It is known that in $Sr_3Ru_2O_7$, rotation of the RuO_6 octahedra causes a symmetry reduction (from $I4/mmm$ to $Pbam$) and the appearance of additional peaks.[7] For $Sr_3Ru_2O_7F_2$, adoption of the space group $Pbam$ resulted in these extra peaks (labeled as O in Fig. 2) being well described, and a much better fit to the pattern was obtained. In the final refinement, a pseudo-Voigt peak profile and 28 points of interpolated background were refined together with structural and other instrumental parameters. The reaction product CuO was incorporated as a secondary phase in the refinement. Only three peak profile parameters were refined for CuO owing to its very broad and low intensity peaks in the pattern. When the constraint on the phase fraction was

TABLE II. Selected bond lengths (Å) and bond angles of $Sr_3Ru_2O_7F_2$

Bonds	At 290 K		At 2 K	
Sr1–O1×2	2.712(1)	2.708(1)	2.705(1)	2.701(1)
Sr1–O5×4	2.516(2)	3.000(2)	2.504(2)	3.020(3)
Sr2–O2×2	2.712(1)	2.708(1)	2.705(1)	2.701(1)
Sr2–O6×4	2.585(3)	3.164(4)	2.578(4)	3.160(4)
Sr3–O3×2	2.760(2)	2.763(2)	2.753(1)	2.756(1)
Sr3–O5×2	2.942(4)	3.365(3)	2.910(4)	3.364(3)
Sr3–F×2	2.563(3)	2.444(3)	2.561(3)	2.441(3)
Sr4–O4×2	2.788(2)	2.791(2)	2.780(2)	2.784(4)
Sr4–O6×2	2.883(5)	3.412(4)	2.882(5)	3.414(4)
Sr4–F×2	2.328(3)	2.508(4)	2.312(3)	2.505(3)
Ru1–O1	2.093(3)	. . .	2.090(3)	. . .
Ru1–O3	1.833(8)	. . .	1.824(7)	. . .
Ru1–O5×2	1.948(7)	1.955(7)	1.941(5)	1.960(5)
Ru2–O2	2.042(3)	. . .	2.046(3)	. . .
Ru2–O4	1.888(7)	. . .	1.887(7)	. . .
Ru2–O6×2	1.966(1)	1.967(1)	1.962(1)	1.961(1)
Ru1–O5–Ru1	. . .	158.1°(1)	. . .	156.9°(1)
Ru2–O6–Ru2	. . .	154.1°(2)	. . .	153.9°(2)

released, the correct ratio of CuO to the main phase $Sr_3Ru_2O_7F_2$ (1.02:1) was obtained. In the refinement, the oxygen position in the middle double layer (Fig. 3) had to be split into two positions similar to that reported by Huang *et al.*[7] for $Sr_3Ru_2O_7$. This indicates that whereas the RuO_6 octahedra rotations of adjacent layers within a double layer are correlated, those between the double layers are not. No significant oxygen or fluorine deficiencies were observed in any of the atomic sites, which is consistent with our TGA results. The latter gave an oxygen content of 7.03(3), which also agrees very well with the ideal chemical formula $Sr_3Ru_2O_7F_2$. The final refined structure parameters are listed in Table I. The important bond lengths and angles are listed in Table II.

The layer sequence of the $Sr_3Ru_2O_7F_2$ structure can be described as

$$\overbrace{SrO-RuO_2-SrO-F_2-SrO-RuO_2-SrO}^{c/2}$$

compared to the $Sr_3Ru_2O_7$ structure[7]

$$\overbrace{SrO-RuO_2-SrO-SrO-RuO_2-SrO}^{c/2}.$$

This clearly shows that $Sr_3Ru_2O_7F_2$ can be derived from the double layer $Sr_3Ru_2O_7$ by inserting F atoms into the rock salt SrO layers. The inserted F occupies the tetrahedral holes formed by four neighboring Sr atoms. Fluorine insertion decouples the apical O coordination to Sr3 and Sr4 atoms and now Sr3 and Sr4 are linked to 4 F atoms instead, leaving all the Sr atoms to be 12 coordinated (Sr1,Sr2–12O, Sr3,Sr4–8O+4F). The Sr–O and Sr–F bond lengths are close to those reported in related compounds, e.g., $SrRuO_3$ (2.505–3.123 Å),[12] Sr_2RuO_4 (2.428–2.744 Å),[13] and $Sr_3Ru_2O_7$ (2.459–2.962 Å),[7] and SrF_2 (2.511 Å). The in plane Ru–O bonds and the Ru–O apical bonds pointing to the central O atoms within the double layer are also common to the related layered ruthenates. However, there is a pronounced contraction in the external Ru–O apical bonds pointing toward the F2 layer (Ru1–O3, 1.833 Å and Ru2–O4, 1.888 Å) in $Sr_3Ru_2O_7F_2$ compared with the equivalent bonds in $Sr_3Ru_2O_7$ (2.025 Å). This change is consistent with oxidation from Ru^{4+} in $Sr_3Ru_2O_7$ to Ru^{5+} in $Sr_3Ru_2O_7F_2$.

At low temperature (2 K), additional weak peaks are present at high d values, i.e., $d=5.28$ Å, $d=4.95$ Å, and $d=4.50$ Å (Fig. 4), which indicated magnetic order and could be indexed with the same unit cell as the major peaks. Pattern simulation showed that the peaks are consistent with a *G*-type magnetic structure with magnetic moment along the *c* direction, similar to that observed in $Sr_3Mn_2O_7$.[14] Structure refinement at 2 K was performed in a similar fashion to that at 290 K, except that here the lattice constants of CuO were also refined. The refined CuO cell [$a=4.665(1)$ Å, $b=3.418(1)$ Å, $c=5.134(2)$ Å, and $\beta=99.06°(3)$], is in accord with reported low temperature NPD results.[15] It is worth noting that the orthorhombic distortion of $Sr_3Ru_2O_7F_2$ at 2 K is only slightly enhanced as one can see from the change of lattice constants. There are no dramatic changes in the bond lengths between Sr–O, Sr–F, and Ru–O either,

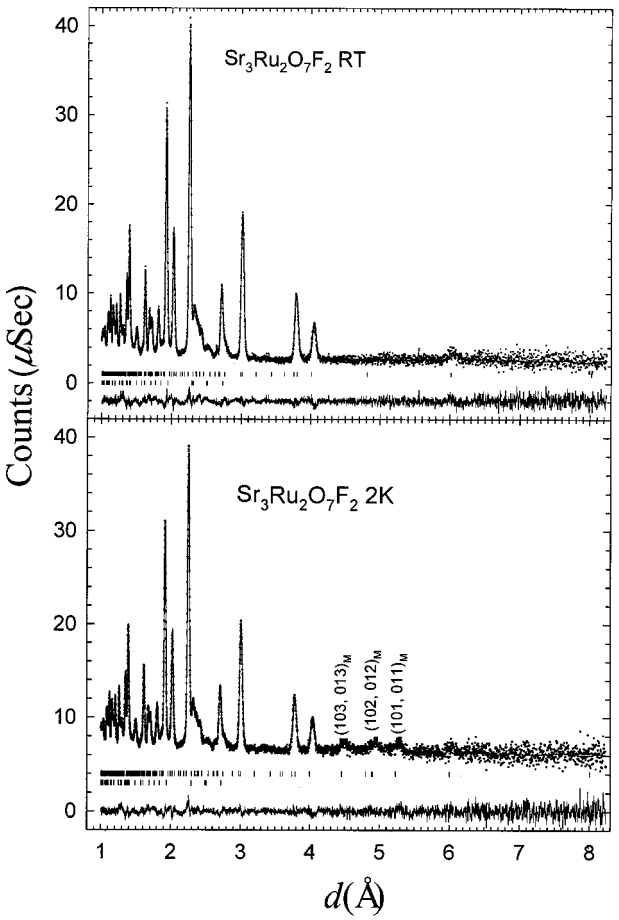

FIG. 4. Neutron diffraction patterns (A-Bank) of $Sr_3Ru_2O_7F_2$ at 290 K (top) and 2 K (bottom): (dots) calculated, (lines) observed and difference, the vertical marks represent the allowed diffraction peaks for $Sr_3Ru_2O_7F_2$ (upper) and CuO (lower).

indicating the changes are purely due to thermal expansion and no structural transition takes place between 290 and 2 K.

Because there is no reliable form factor for the Ru^{5+} ion,[16] we have taken the values for the Ru^{1+} ion, which gives a magnetic moment of $1.05(7)\mu_B$/Ru. It is known that the form factor of higher valent state of an ion decays more slowly with $\sin\theta/\lambda$ than lower valent states. If we adopt the form factor of V^{2+}, which has the same d^3 electronic state but decays much slower then Ru^{1+}, a moment of $0.98(6)\mu_B$/Ru is obtained. Since the form factor of the $4d^3$ ion will decay faster than that of the $3d^3$ ion, it is clear that the magnetic moment of Ru in $Sr_3Ru_2O_7F_2$ will be between the two refined values, that is around $1\mu_B$/Ru. There may be several reasons for the reduction in moment below the ideal value, $3\mu_B$/Ru. First, the strong covalency of the Ru^{5+}–O bond will decrease the localized moment on Ru. Second, the two-dimensional nature will also reduce the moment due to zero-point fluctuations. Related to the above, there may also be mobile electrons moving in the Ru4d_{xy}–O2p_π–Ru4d_{xy} orbitals, which again suppress the localized moment on Ru. The observation of a FM moment below 185 K in the sample may be due to the Dzyaloshinsky–Moriya (DM) spin canting mechanism, and it is indeed allowed in the orthorhombic lattice. However, due to the small FM moment ($\sim 0.02\mu_B$/Ru), the direction (within the ab plane if the DM mechanism applies) and magnitude cannot be determined in the present NPD refinement.

It is known that rotation of transition metal oxygen octahedra has a major effect on the electron transfer bandwidth of perovskite related oxides. The rotation angles for $Ru1-O_6$ (11° at 290 K, 11.6° at 2 K) and $Ru2-O_6$ (13° at 290 K, 13.1° at 2 K) octahedra are significantly larger than those in $Sr_3Ru_2O_7$ [7.2° at room temperature (RT), 8.0° at 9 K][7] and may be comparable with those in a related double layer compound $Sr_3Ir_2O_7$ (11.8° at RT).[17] A reduction of bandwidth can be expected in the fluorinated compound due to such a large RuO plane distortion. Given that the Ru^{5+} valent state in $Sr_3Ru_2O_7F_2$ will result in an exact half filling of the t_{2g} orbitals, both factors will favor the AFM ordering between Ru ions through $Rut_{2g}-O2p_{\pi}-Rut_{2g}$ superexchange interactions.

In conclusion, we have succeeded in preparing a new layered ruthenate which is derived from the double layer R–P phase, $Sr_3Ru_2O_7$, by F insertion between the SrO layers. Large rotations of the RuO_6 octahedra within the Ru–O planes were revealed from the NPD structure refinements. The Ru magnetic moments order antiferromagnetically along the *c* axis at low temperature with a *G*-type structure. The FM transition at 185 K may be attributed to canting of the moments to produce a component in the *ab* plane. However, we do not have a satisfactory explanation of the high ordering temperature observed for $Sr_3Ru_2O_7F_2$. It is higher than any strontium ruthenium oxide, and may relate to the high covalence in this Ru^{5+} material, which would give a high level of π character to the Ru–O bonding.

ACKNOWLEDGMENT

We are grateful to EPSRC for funding this work and providing ND facilities.

[1] A. Callaghan, C.W. Moeller, and R. Ward, Inorg. Chem. **5**, 1572 (1966).
[2] Y. Maeno, H. Hashimota, K. Yoshida, S. Nishizaki, T. Fujita, J.G. Bednorz, and F. Lichtenberg, Nature (London) **372**, 532 (1994).
[3] T.M. Rice, and M. Sigrist, J. Phys.: Condens. Matter **7**, L643 (1995).
[4] G. Cao, S. McCall, and J.E. Crow, Phys. Rev. B **55**, R672 (1997).
[5] Y. Maeno, S. Nakatruji, and S. Ikeda, Mater. Sci. Eng., B **63**, 70 (1999).
[6] R.J. Cava, H.W. Zandbergen, J.J. Krajewski, W.F. Peck, Jr., B. Batlogg, S. Carter, R.M. Fleming, O. Zhao, and L.W. Rupp, Jr., J. Solid State Chem. **116**, 141 (1995).
[7] Q. Huang, J.W. Lynn, R.W. Erwin, J. Jarupatrakorn, and R.J. Cava, Phys. Rev. B **58**, 8515 (1998).
[8] G. Cao, S. McCall, J.E. Crow, and R.P. Gurtin, Phys. Rev. B **56**, 5387 (1997).
[9] M. Al-Mamouri, C. Greaves, P.P. Edwards, and M. Slaski, Nature (London) **369**, 382 (1994).
[10] C. Greaves, J.L. Kissick, M.G. Francesconi, L.D. Aikens, and L.J. Gillie, J. Mater. Chem. **9**, 111 (1999).
[11] A.C. Larson and R.B. von Dreele, *General Structure Analysis System* (Los Alamos National Lab, Los Alamos, NM, 1994).
[12] C.W. Jones, P.D. Battle, P. Lightfoot, and W.T. Harrison, Acta Crystallogr., Sect. C: Cryst. Struct. Commun. **45**, 365 (1989).
[13] T. Vogt and D.J. Buttrey, Phys. Rev. B **52**, R9843 (1995).
[14] J.F. Mitchell, J.E. Millburn, M. Medarde, S. Short, J.D. Jorgensen, and M.T. Fernandez-Diaz, J. Solid State Chem. **141**, 599 (1998).
[15] N.E. Bresse, M. O'Keeffe, B.L. Ramakrishna, and R.B. von Dreele, J. Solid State Chem. **89**, 184 (1990).
[16] P.J. Brown, in *International Tables for Crystallography*, edited by A.J. Wilson (Kluwer Academic, Dordrecht, 1992), Vol. C, pp. 391, 512.
[17] M. Subramanian, M.K. Crawford, and R.L. Harlow, Mater. Res. Bull. **29**, 645 (1994).